ELSEVIER

Journal of Nuclear Materials 250 (1997) 88–95

journal of nuclear materials

Melting behaviour of oxide systems for heterogeneous transmutation of actinides.

III. The system Am–Mg–O

Hengzhong Zhang [1], R.J.M. Konings *, M.E. Huntelaar, E.H.P. Cordfunke

Netherlands Energy Research Foundation ECN, P.O.Box 1, 1755 ZG Petten, The Netherlands

Received 22 July 1997; accepted 18 September 1997

Abstract

Unknown thermodynamic data of a number of americium oxides were estimated. Phase diagrams of related binary and ternary systems in the Am–Mg–O system were calculated by transposing solution model parameters of the Pu–Mg–O system to the Am–Mg–O system. According to the calculated results, the liquid phase in the MgO–AmO_{2-x} system starts to form at 1930 K in the oxygen pressure range 4.3×10^{-7} to 4.5 bar, and at the temperature varying from 2221 K to 2356 K at an oxygen pressure higher than 4.5 bar. © 1997 Elsevier Science B.V.

1. Introduction

Magnesium oxide (MgO) is considered to be a promising support material (inert matrix) for heterogeneous transmutation of actinides, such as plutonium and americium, in fast nuclear reactors, since it has a high melting point (3100 K) and a relatively high thermal conductivity [1]. The temperature at which a liquid starts to form in the MgO–PuO_{2-x} system is higher than 2341 K according to phase diagram calculations presented before [2], which shows that MgO is in potential a good matrix material for the heterogeneous transmutation of plutonium. Nevertheless, a good understanding of the melting behaviour of the MgO–AmO_{2-x} system has not been reached yet. In the present work, the melting behaviour of the MgO–AmO_{2-x} system will be studied using the phase diagram calculation method.

The Am–O system is a basic system in assessing the melting behaviour of the MgO–AmO_{2-x} system. It has been reviewed in Refs. [3–5]. At high temperatures, there are two phases present in the Am–O system: the hexagonal (hex) $AmO_{1.5}$ phase and the fcc AmO_{2-x} phase ($1.62 \leq 2-x \leq 2$) [3,6]. According to Ahrland et al. [4], the phase diagram of the Am–O system is similar to that of the Pu–O system. However, there are still many assumptions on the phase relations.

For the MgO–AmO_{2-x} system only the subsolidus phase relations have been studied [7,8], melting information is not available. For the simplicity and because the experimental information about the high-temperature phase relations is not available, the two limiting boundary phases of the fcc AmO_{2-x} phase, $AmO_{1.62}$ and AmO_2, are treated as two line compounds. As a result, the MgO–AmO_{2-x} system can be treated as two subsystems, the MgO–$AmO_{1.5}$–$AmO_{1.62}$ system and the MgO–$AmO_{1.62}$–AmO_2 system in phase diagram calculations. The melting behaviour of the MgO–AmO_{2-x} system will be obtained from the calculations.

---

* Corresponding author. Tel.: +31-224 564 138; fax: +31-224 563 608; e-mail: konings@ecn.nl.

[1] Visiting scientist on leave from Department of Chemistry, Central South University of Technology, Changsha, Hunan 410083, People's Republic of China.

PII S0022-3115(97)00290-0

2. Thermodynamic data of oxides

The thermodynamic data from SGTE were selected for the halite MgO phase and the liquid MgO phase [9]; the data for the metastable fcc MgO phase are from Ref. [10].

The thermodynamic data for the americium oxides are very uncertain. The data for $AmO_{1.5}$ (solid) and AmO_2 (solid) have been presented in the recent NEA/OECD review by Silva et al. [5], but are, except the enthalpies of formation, based on estimates. These data have been used here. Thermodynamic data for $AmO_{1.5}$(liquid), AmO_2(liquid) and $AmO_{1.62}$ cannot be found in literature; their thermodynamic properties have therefore been estimated in the present work, as presented in Section 3. These estimates are subjected to large uncertainties and are in some instances speculative.

3. Estimation of thermodynamic data of americium oxides

3.1. *$AmO_{1.5}$(liquid) and AmO_2(liquid)*

The melting point of $AmO_{1.5}$ was determined to be (2478 ± 15) K; from extrapolation of melting point data of other actinide dioxides (see Table 1), the melting point of AmO_2 was estimated to be 2448 K [3].

In order to estimate the properties of $AmO_{1.5}$(liquid) and AmO_2(liquid), we take the mean value (2.877) of $\Delta_{fus} H^0/RT_m$ of $CeO_{1.5}$ and $PuO_{1.5}$ as that of $AmO_{1.5}$ and presume $\Delta_{fus} H^0/RT_m = 3.0$ for AmO_2 as is valid for the values of UO_2 and PuO_2 (Ref. [2]). Thus,

$$\Delta_{fus} H^0(AmO_{1.5}) = 2.877 RT_m$$

$$= (59 \pm 20)\ \text{kJ mol}^{-1}, \tag{1}$$

$$\Delta_{fus} H^0(AmO_2) = 3.0 RT_m = (61 \pm 20)\ \text{kJ mol}^{-1}. \tag{2}$$

In Eqs. (1) and (2), the uncertainties of $\Delta_{fus} H^0$ are assigned 20 kJ mol^{-1} assuming the same values as in Ref. [2]. The entropies of fusion of $AmO_{1.5}$ and AmO_2 are then calculated to be (24 ± 8) and (25 ± 8) J K^{-1} mol^{-1}, respectively.

As an approximation, we assume that the heat capacities of $AmO_{1.5}$(liquid) and AmO_2(liquid) have the same values as $PuO_{1.5}$(liquid) and PuO_2(liquid), respectively (see Table 1).

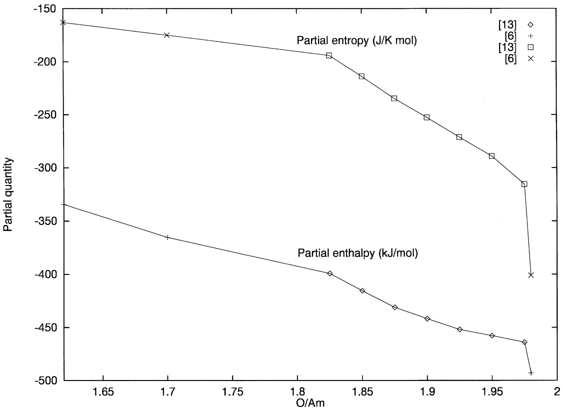

Fig. 1. Variations of $\Delta \overline{H}(O_2)$ and $\Delta \bar{S}(O_2)$ of AmO_{2-x} with the oxygen content.

3.2. *$AmO_{1.62}$(solid, fcc)*

The thermodynamic functions of $AmO_{1.62}$ can be derived from the oxygen potential data of AmO_{2-x} in Refs. [6,13] using the method described by Zhang et al. [14]. Fig. 1 illustrates the variations of $\Delta \overline{H}(O_2)$ and $\Delta \bar{S}(O_2)$ with the oxygen content.

Numerical integration of the partial quantities of oxygen of AmO_{2-x} were performed with respect to the oxygen content ($n = 2 - x = O/Am$). Regression of Eqs. (3) and (4) represent the integrated results:

$$\int_{1.62}^{n} \Delta \overline{H}(O_2)\, dn/\text{kJ mol}^{-1} = 16.1 + 308.3n - 196.5n^2, \tag{3}$$

$$\int_{1.62}^{n} \Delta \bar{S}(O_2)\, dn/\text{J K}^{-1}\text{mol}^{-1} = -384.6 + 601.2n$$

$$-224.8n^2. \tag{4}$$

From Eqs. (3) and (4), we obtain $\int_{1.62}^{2} \Delta \overline{H}(O_2)\, dn = -153.3$ kJ mol^{-1} and $\int_{1.62}^{2}$ $\Delta \bar{S}(O_2)\, dn = -81.5$ J $K^{-1} \cdot mol^{-1}$.

Table 1
Melting properties of several oxides

Oxide	$CeO_{1.5}$	$PuO_{1.5}$	$AmO_{1.5}$	UO_2	PuO_2	AmO_2
T_m (K)	2513	2358 ± 25	2478 ± 15	3140	2663	2448
$\Delta_{fus} H^0/RT_m$	2.872	2.882	2.877[a]	2.988	3.026	3.0[a]
C_p^0(liquid) (J K^{-1} mol^{-1})	100.0	100.0	100.0[a]	131.0	131.0	131.0[a]
Ref.	[11]	[12]	[3]	[11]	[11]	[3]

[a] Estimated in the present work.

According to Zhang et al. [14], the enthalpy and the entropy of $AmO_{1.62}$ can be derived from those of AmO_2 [5]:

$$\begin{aligned}&\Delta_f H^0[AmO_{1.62}(s),\ 298.15\ K]\\ &\quad = \Delta_f H^0[AmO_2(s),\ 298.15\ K] + \frac{1}{2}\int_2^{1.62} \Delta \bar{H}(O_2)\, dn\\ &\quad = (-932.3 \pm 3.0) + \frac{1}{2}[-(-153.3)]\\ &\quad = (-855.6 \pm 3.0)\ kJ\ mol^{-1} \qquad (5)\end{aligned}$$

$$\begin{aligned}&S^0[AmO_{1.62}(s), 298.15\ K]\\ &\quad = S^0[AmO_2(s), 298.15\ K]\\ &\qquad + \frac{1}{2}\int_2^{1.62} \Delta \bar{S}(O_2)\, dn\\ &\qquad + \frac{(1.62-2)}{2} S^0[O_2(g),\ 298.15\ K]\\ &\quad = (67 \pm 10) + \frac{(1.62-2)}{2} 205.04 + \frac{1}{2}[-(-81.5)]\\ &\quad = (69 \pm 10)\ J\ K^{-1}\, mol^{-1} \qquad (6)\end{aligned}$$

The heat capacity of the fcc AmO_{2-x} phase can be derived from that of AmO_2 (298.15–2000 K) [5]:

$$C_p^0(AmO_n(s))/J\ K^{-1}\ mol^{-1} = C_p^0(AmO_2) + \frac{n-2}{2} \times C_p^0[O_2(gas)]. \qquad (7)$$

When $n = 1.62$, Eq. (7) yields

$$\begin{aligned}&C_p^0(AmO_{1.62}(s))/J\ K^{-1}\ mol^{-1}\\ &\quad = 79.048 + 9.925 \times 10^{-3} T\\ &\quad - 18.967 \times 10^5 T^{-2} - 8.159 \times 10^{-7} T^2. \qquad (8)\end{aligned}$$

3.3. *AmO$_{1.62}$(liquid)*

No information on the melting behaviour of $AmO_{1.62}$ has been reported in literature. However, some information can be deduced from the measurements of the melting temperature (T_m) of the AmO_2 samples at various heating rates as reported in by McHenry [15] (see Table 2). Because AmO_2 can lose oxygen [7] at high temperatures, the oxygen content of the samples will be determined by the heating rate of the measurements: the lower the heating rate (as a result of which the time for the measurement is longer), the less the oxygen content. Table 2 shows that there is a steep decrease in T_m at the rate below 20 to 30 K min^{-1}. It is very probable that at such a rate the AmO_2 sample actually approached the low oxygen limit phase ($AmO_{1.62}$) in the homogeneous field of the fcc AmO_{2-x} phase. On the other hand, since the Am–O system is similar to the Pu–O system, a eutectic point between $AmO_{1.5}$(hex) and AmO_{2-x}(fcc) can be expected. Thus the T_m of the AmO_2 sample obtained with the very low rate (0.3 to 3 K min^{-1}) is very probably the eutectic temperature between $AmO_{1.5}$ and $AmO_{1.62}$. Based on the assumptions made above, the following hypotheses are made:

Table 2
The melting temperature of AmO_2 sample at various heating rates [15]

Heating rate (K min^{-1})	T_m (K)	Atmosphere
0.3	2023	He
3	2053	He
20	2333	He
30	2323	He, air
150	2393	He

- T_m of the AmO_2 sample at the rate (20 to 30 K min^{-1}) is that of $AmO_{1.62}$. The mean value (2328 K) at the two rates is taken as $T_m(AmO_{1.62})$.
- T_m of the AmO_2 sample at the rate (0.3 ~ 3 K min^{-1}) is the eutectic temperature of the $AmO_{1.5}$–$AmO_{1.62}$ system. The mean value (2038 K) at the two rates is taken as T_{eut}.

A linear interpolation between the $\Delta_{fus} H^0/RT_m$ values of $AmO_{1.5}$ and AmO_2 is used to estimate that of $AmO_{1.62}$, which gives the value 2.91. Thus,

$$\begin{aligned}&\Delta_{fus} H^0(AmO_{1.62}) = 2.91\, RT_m\\ &= (56 \pm 20)\ kJ\ mol^{-1} \qquad (9)\end{aligned}$$

where the uncertainty of $\Delta_{fus} H^0$ is assigned the same value as in Eq. (1). The entropy of fusion of $AmO_{1.62}$ is thus calculated to be (24 ± 8) J K^{-1} mol^{-1}. The heat capacity of $AmO_{1.62}$(liquid) can be approximated by that of $PuO_{1.61}$ (liquid), 125 J K^{-1} mol^{-1} [2].

4. Phase diagram calculations

For the phase diagram calculations, the MTDATA program [16] was used. Ternary phase diagrams of the MgO–$AmO_{1.5}$–$AmO_{1.62}$ system and the MgO–$AmO_{1.62}$–AmO_2 system were calculated using the Muggianu method [17] based on the solution model parameters of their three composing binary systems. It should be stressed that in view of the uncertainties in the data of the thermodynamic properties of the americium oxides, the phase diagrams presented below should be considered as tentative.

4.1. *Binary systems*

4.1.1. *AmO$_{1.62}$–AmO$_2$*

The solid solution of the $AmO_{1.62}$–AmO_2 system is actually the non-stoichiometric fcc AmO_{2-x} phase (1.62

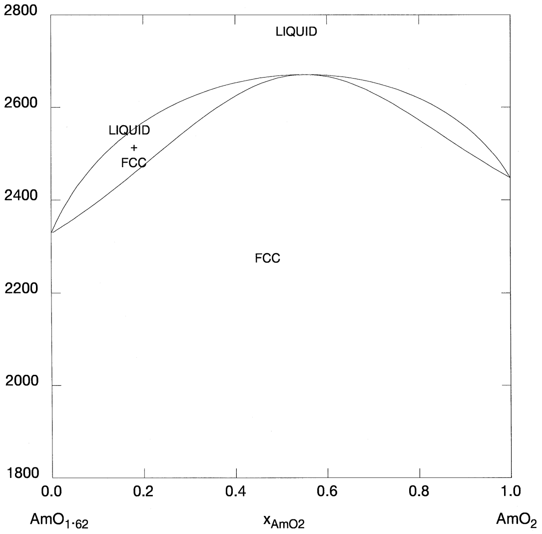

Fig. 2. Calculated phase diagram of the system $AmO_{1.62}-AmO_2$.

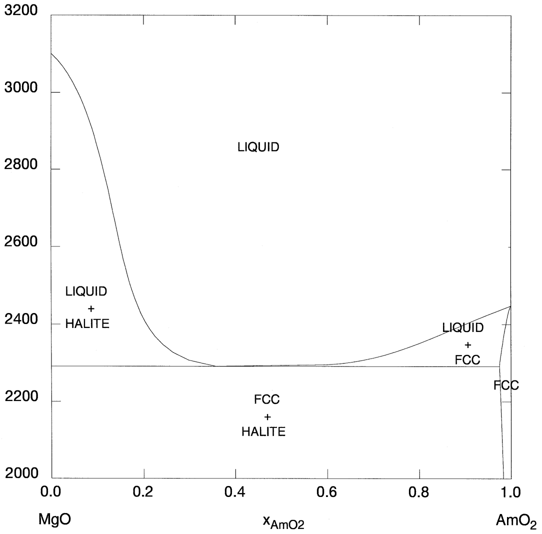

Fig. 4. Calculated phase diagram of the system $MgO-AmO_2$.

$\leq 2 - x \leq 2$). The enthalpy and entropy of the AmO_{2-x} phase can be correlated to the oxygen content according to Ref. [14] with equations similar to Eqs. (5) and (6). The heat capacity can be obtained according to Eq. (7). Thus, the Gibbs energy of AmO_{2-x} can be calculated. The liquid phase of the $AmO_{1.62}$–AmO_2 system was assumed ideal considering the fact that the two liquid components have only a small difference in the oxygen contents. As a result, the phase diagram of the $AmO_{1.62}$–AmO_2 system was calculated (Fig. 2). At 55 mol% AmO_2 or $O/Am = 1.83$, there is a maximum (2670 K) in the liquidus and solidus curves.

4.1.2. $AmO_{1.5}$–$AmO_{1.62}$

Because the Am–O system is assumed to be similar to the Pu–O system [4], the $AmO_{1.5}$–$AmO_{1.62}$ system can also be treated as a simple eutectic like the $PuO_{1.5}$–$PuO_{1.61}$ system [2]. The liquid phase was modelled as a regular solution by trial and errors (Ref. [18]). The calculated

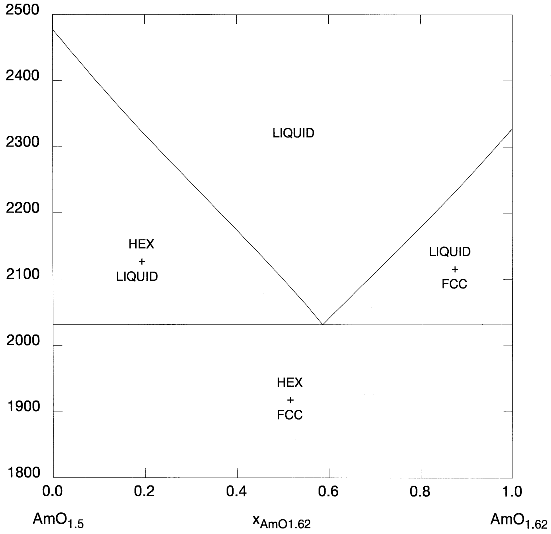

Fig. 3. Calculated phase diagram of the system $AmO_{1.5}-AmO_{1.62}$.

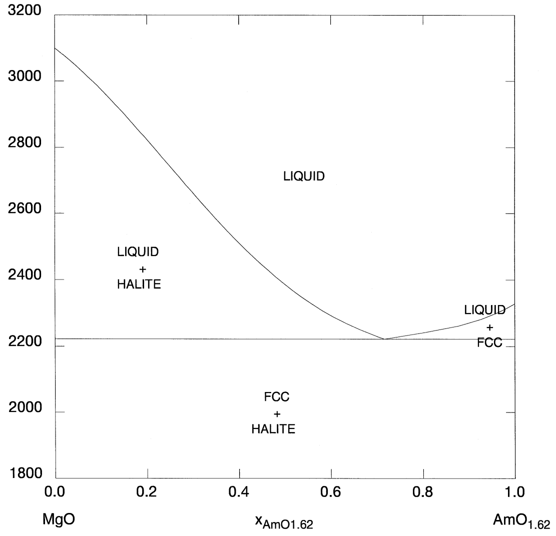

Fig. 5. Calculated phase diagram of the system $MgO-AmO_{1.62}$.

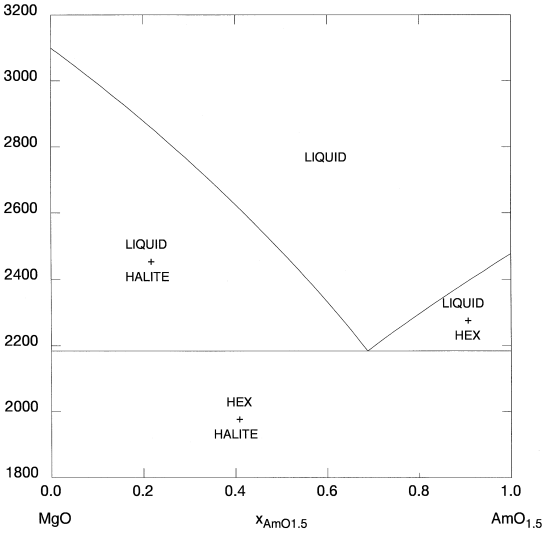

Fig. 6. Calculated phase diagram of the system MgO–$AmO_{1.5}$.

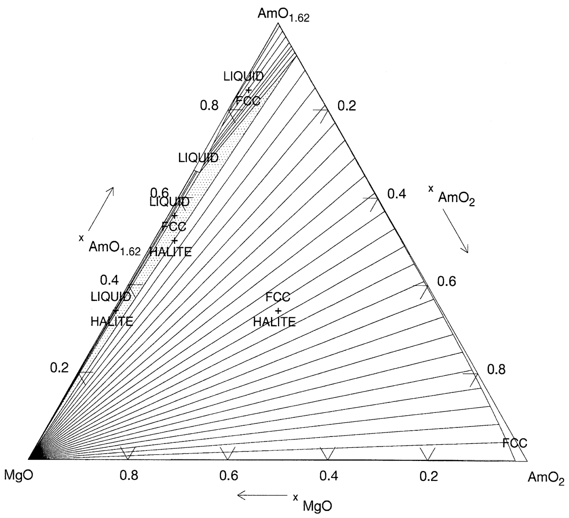

Fig. 8. Calculated phase diagram of the system MgO–$AmO_{1.62}$–AmO_2 at 2250 K.

phase diagram is shown in Fig. 3. The calculated eutectic temperature (2031 K at 59 mol% $AmO_{1.62}$ or O/Am = 1.57) is close to the hypothetical value 2038 K (see Section 3.3).

4.1.3. MgO–AmO_2

It is assumed that the phase diagram of the MgO–AmO_2 system is similar to that of the MgO–PuO_2 system because AmO_2 and PuO_2 have similar properties. Thus the solution model parameters of the fcc phase and the liquid phase in the MgO–PuO_2 system were directly transposed to the MgO–AmO_2 system (Ref. [18]). The calculated phase diagram is shown in Fig. 4. The calculated eutectic point is at 2291 K and 36 mol% AmO_2.

4.1.4. MgO–$AmO_{1.62}$

The phase diagram of the MgO–$AmO_{1.62}$ system is assumed a simple eutectic similar to that of the MgO–$PuO_{1.61}$ system [2]. By transposing the solution model parameters of the liquid phase in the MgO–$PuO_{1.61}$ system to the MgO–$AmO_{1.62}$ system (Ref. [18]), the phase diagram of the MgO–$AmO_{1.62}$ system was calculated, as

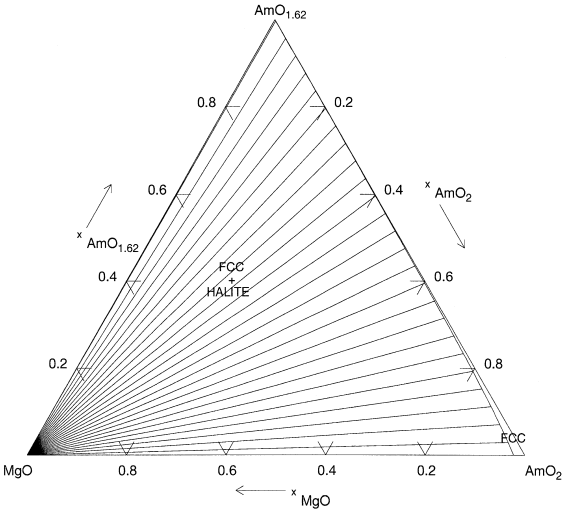

Fig. 7. Calculated phase diagram of the system MgO–$AmO_{1.62}$–AmO_2 at 2200 K.

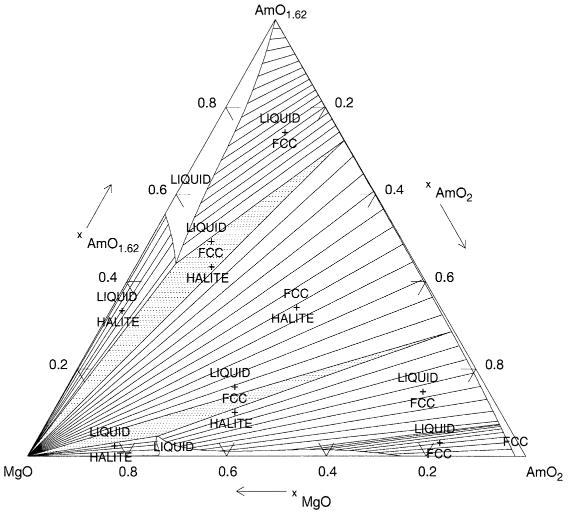

Fig. 9. Calculated phase diagram of the system MgO–$AmO_{1.62}$–AmO_2 at 2330 K.

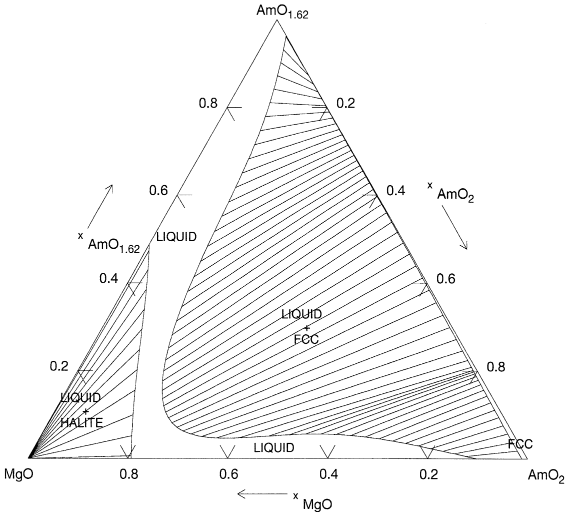

Fig. 10. Calculated phase diagram of the system MgO–$AmO_{1.62}$–AmO_2 at 2400 K.

shown in Fig. 5. The calculated eutectic point is at 2221 K and 71 mol% $AmO_{1.62}$.

4.1.5. MgO–$AmO_{1.5}$

MgO and $AmO_{1.5}$ are insoluble according to Ref. [7]. By assuming an ideal liquid solution in the system, the phase diagram of the system was calculated, as shown in Fig. 6. The calculated eutectic point is at 2184 K and 69 mol% $AmO_{1.5}$.

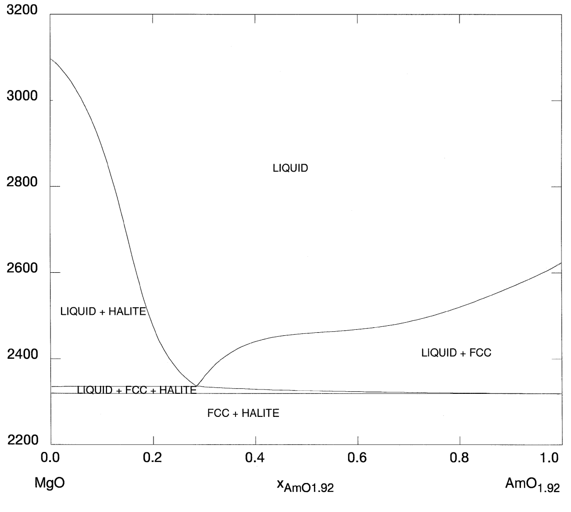

Fig. 11. Isopleth $T-x$ diagram of the pseudo-binary MgO–$AmO_{1.92}$ system.

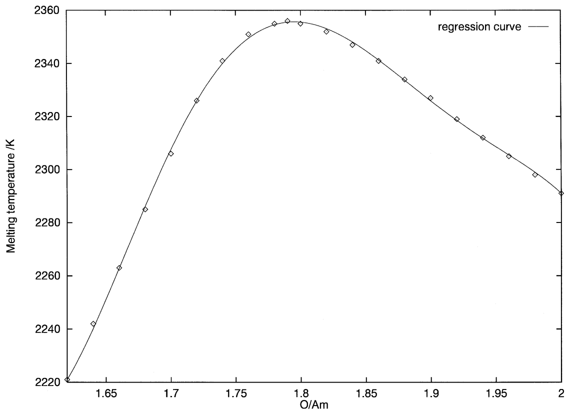

Fig. 12. Variation of the 'melting temperature' with the oxygen content in the MgO–AmO_{2-x} system $(1.62 \leq 2-x \leq 2)$.

4.2. Ternary systems

4.2.1. MgO–$AmO_{1.5}$–$AmO_{1.62}$

The phase diagram of this system is a simple ternary eutectic according to the calculation. The calculated ternary eutectic point is at 1930 K, 18 mol% MgO, 41 mol% $AmO_{1.5}$ and 41 mol% $AmO_{1.62}$.

4.2.2. MgO–$AmO_{1.62}$–AmO_2

Isothermal phase diagrams of the system were calculated at various temperatures. Figs. 7–10 show the calculated isothermal sections of the system at 2200 K, 2250 K, 2330 K and 2400 K, respectively. It can be seen from these diagrams that

- at 2200 K, there is no liquid is formed in the system;
- at 2250 K, liquid occurs at the MgO–$AmO_{1.62}$ side;
- at 2330 K, liquids form from both the MgO–$AmO_{1.62}$ and the MgO–AmO_2 sides;
- at 2400 K, the two liquid fields merge to one field.

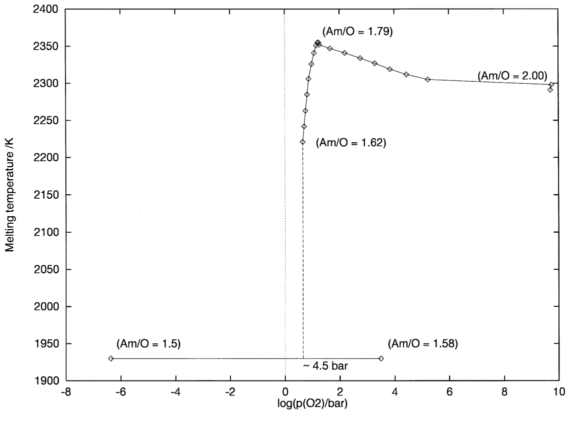

Fig. 13. The 'melting temperature' vs. oxygen potential of the MgO–AmO_{2-x} system.

5. Melting behaviour in the MgO–AmO_{2-x} system

From the results presented in the previous section, the melting behavior of the MgO–AmO_{2-x} system can be derived, as will be discussed below. In this section the temperature at which the first liquid occurs is referred to as the ‘melting temperature’ (T_m) of the system, which can be the solidus or the eutectic temperature.

5.1. MgO–AmO_{2-x} ($1.5 \leq 2-x \leq 1.62$)

Because the MgO–$AmO_{1.5}$–$AmO_{1.62}$ system is a simple ternary eutectic, the liquid phase starts to form when the temperature reaches the ternary eutectic temperature, 1930 K. Thus, $T_m = 1930$ K for the MgO–AmO_{2-x} system when ($1.5 \leq 2-x \leq 1.62$).

5.2. MgO–AmO_{2-x} ($1.62 \leq 2-x \leq 2$)

From isopleth T–x phase diagram calculations of the MgO–$AmO_{1.62}$–AmO_2 system, T_m of the MgO–AmO_{2-x} system when ($1.62 \leq 2-x \leq 2$) can be obtained. Fig. 11 shows the isopleth T–x phase diagram of the pseudo-binary system MgO–$AmO_{1.92}$, according to which the liquid phase starts to form at 2319 K.

The variation of T_m with the oxygen content of AmO_{2-x} is shown in Fig. 12 and is represented by the following regression equation:

$$T_m = 2221(1-N) + 2291N + N(1-N) \times [236.6 + 1578.6N - 3478.0N^2 + 1908.8N^3], \quad (10)$$

where

$$N = [(O/Am) - 1.62]/0.38 \quad (1.62 \leq O/Am \leq 2). \quad (11)$$

6. Discussion and conclusion

The oxygen potential of a non-stoichiometric oxide can be calculated using the following relation:

$$RT \ln(p(O_2)) = \Delta \bar{H}(O_2) - T\Delta \bar{S}(O_2). \quad (12)$$

$\Delta \bar{H}(O_2)$ and $\Delta \bar{S}(O_2)$ data of AmO_{2-x} ($1.62 \leq 2-x \leq 2$) were reported in Ref. [6,13] (see Fig. 1). Those for $AmO_{1.5}$ and $AmO_{1.58}$ were reported in Ref. [6]. According to Eq. (12), the oxygen potential of AmO_{2-x} can be calculated at the ‘melting temperature’ of the MgO–AmO_{2-x} system. A plot of T_m vs. oxygen potential is shown in Fig. 13.

Fig. 13 shows that, at an oxygen pressure between 4.3×10^{-7} bar and 4.5 bar, T_m of the MgO–AmO_{2-x} system remains at 1930 K. When $p(O_2) \geq 4.5$ bar, $AmO_{1.62}$ becomes stable, T_m increases rapidly. When the oxygen potential increases further, T_m reaches a maximum (2356 K) at $p(O_2) = 10.6$ bar, and then decreases almost linearly up to $p(O_2) = 1.6 \times 10^5$ bar. After that, T_m remains at about 2300 K. In the experimental work [7] the thermal processing of the MgO + AmO_2 samples were all below 1923 K which is close to but below the lowest T_m value (1930 K), thus only the subsolidus phase relations could be determined. Moreover, because the fcc phase field [MgO(fcc) + AmO_{2-x}(fcc)] in the MgO–AmO_{2-x} system is very narrow (see Figs. 7–10), it is clear that no mutual solid solubility between MgO and AmO_2 was detected in the experiment [7].

According to the above discussion, when using MgO as a support material for the transmutation of americium,

- the ‘melting temperature’ of the MgO–AmO_{2-x} system is very low (1930 K) at partial oxygen pressures below 1 bar;
- very high oxygen potentials are needed to raise the ‘melting temperature’ above a required value (e.g. ≥ 4.5 bar for a temperature of 2220 K). However, at these oxygen potentials, corrosion of cladding materials of fuel rods can easily occur.

As a result, it is doubtful whether MgO is a good support material for the transmutation of americium.

References

[1] N. Cocuaud, E. Picard, R.J.M. Konings, A. Conti, Hj. Matzke, Procceedings Global’97, Yokohama, Oct. 1997, p. 1044.
[2] H. Zhang, M.E. Huntelaar, R.J.M. Konings, E.H.P. Cordfunke, J. Nucl. Mater. 249 (1997) 223.
[3] W.W. Schulz, The Chemistry of Americium, ERDA Technical Information Centre, Oak Ridge, TN, 1976, p. 152.
[4] S. Ahrland, K.W. Bagnall, D. Brown, R.M. Dell, S.H. Ererle, C. Keller, J.A. Lee, J.O. Liljenzin, P.G. Mardon, J.A.C. Marples, G.W.C. Milner, G. Phillips, P.E. Potter, J. Rydberg, The Chemistry of Actinides, Pergamon, Oxford, 1975, p. 240.
[5] R.J. Silva, G. Bidoglio, M.H. Rand, P.B. Robouch, H. Wanner, I. Puigdomenech, Chemical Thermodynamics of Americium, Elsevier, Amsterdam, 1995, p. 89.
[6] S. Casalta, Hj. Matzke, C. Prunier, Proceedings GLOBAL’95, Intern. Conf. on Evaluation of Emerging Nuclear Fuel Cycle Systems, Versailles, France, Sept. 11–14, 1995, p. 1667.
[7] S. Casalta, K. Richter, C. Prunier, Proceedings GLOBAL’95, Int. Conf. on Evaluation of Emerging Nuclear Fuel Cycle Systems, Versailles, France, Sept. 11–14, 1995, p. 1725.
[8] Studies on the Am–O and the AmO_2–MgO systems for transmutation of Am, ITU Annual Report EUR-16368, 1995, p. 111.
[9] B. Hallstedt, J. Am. Ceram. Soc. 75 (1992) 1497.
[10] E.H.P. Cordfunke, M.E. Huntelaar, M.A. Mignanelli, 3th Frame Work Programme of the European Union, 1996, to be published.
[11] E.H.P. Cordfunke, R.J.M. Konings, J. Phase Equil. 14 (1993) 457.
[12] E.H.P. Cordfunke, R.J.M. Konings, Thermochemical Data for Reactor Materials and Fission Products, North-Holland, Amsterdam, 1990.

[13] T.D. Chikalla, L. Eyring, J. Inorg. Nucl. Chem. 29 (1967) 2281.

[14] H. Zhang, P. Zhang, X. Chen, J. Mater. Chem. 6 (1996) 615.

[15] R.E. McHenry, Trans. Am. Nucl. Soc. 8 (1965) 75.

[16] AEA Technology, MTDATA Handbook, 1994.

[17] M. Hillert, Calphad 4 (1980) 1.

[18] H. Zhang, R.J.M. Konings, M.E. Huntelaar, E.H.P. Cordfunke, Melting behaviour of oxide systems for heterogeneous transmutation of actinides, ECN Report ECN-I-96-051, 1996.